

Probing anomalous couplings using di-Higgs production in electron-proton collisions

Mukesh Kumar,^{1,*} Xifeng Ruan,^{2,†} Rashidul Islam,^{3,‡} Alan S. Cornell,^{1,§} Max Klein,^{4,¶} Uta Klein,^{4,**} and Bruce Mellado^{2,††}

¹*National Institute for Theoretical Physics, School of Physics,
School of Physics and Mandelstam Institute for Theoretical Physics,
University of the Witwatersrand, Johannesburg, Wits 2050, South Africa.*

²*University of the Witwatersrand, School of Physics, Private Bag 3, Wits 2050, South Africa.*

³*Department of Physics, University of Calcutta,
92, Acharya Prafulla Chandra Road, Kolkata 700009, India.*

⁴*Oliver Lodge Laboratory, University of Liverpool, Liverpool, United Kingdom.*

Proposed high energy e^-p colliders would provide sufficient energy in a cleaner environment to probe double Higgs production. Using this production channel to analyse the sensitivity in the involved Higgs couplings, we show that the azimuthal angle correlation between missing transverse energy and forward jet is a very good probe for the non-standard CP-even and CP-odd couplings for hhh , hWW and $hhWW$. Furthermore, we give the exclusion limits on these couplings as a function of integrated luminosity at 95% C.L.

PACS numbers: 14.80.Ec, 11.30.Er, 13.60.-r

The Higgs boson, h , the all important building block of the electroweak symmetry breaking (EWSB) mechanism in the Standard Model (SM), had evaded the physics community for nearly half a century. After a series of tedious searches the ATLAS and CMS collaborations announced a discovery [1, 2] which, we hope, is going to fulfil the gaping hole in our understanding of the particle spectrum. Bit by bit, with more and more data arriving, we are consolidating our understanding of this new particle. From the analyses of Run-I of the LHC data we are almost certain that the new particle is *a* Higgs boson. We are almost there. To be certain we need direct experimental verification of its couplings to fermions and gauge bosons, along with its self interactions. Most importantly the measurement of the Higgs self coupling, λ , would provide special significance as it would lay open the hitherto unexplored EWSB mechanism to direct experimental scrutiny [3–6], which in turn will help us establish that a scalar doublet Φ does indeed break the electroweak symmetry spontaneously when it acquires a nonzero vacuum expectation value, v . Moreover, the minimal SM, merely on the basis of the economy of fields and interactions, assumes the existence of only one physical scalar, h , with $J^{PC} = 0^{++}$. Hence, it is our task to ascertain experimentally the spin and CP properties of the new scalar. Only then can we unambiguously establish that it is *the* Higgs boson of the SM.

Theoretically, the Higgs self coupling appears when, as a result of EWSB in the SM, the scalar potential $V(\Phi)$ gives rise to the Higgs self interactions as follows:

$$V(\Phi) = \mu^2 \Phi^\dagger \Phi + \lambda (\Phi^\dagger \Phi)^2 \\ \rightarrow \frac{1}{2} m_h^2 h^2 + \lambda v h^3 + \frac{\lambda}{4} h^4, \quad (1)$$

where $\lambda = \lambda_{\text{SM}} = m_h^2 / (2v^2) \approx 0.13$ and Φ is an $SU(2)_L$ scalar doublet. Clearly, for direct and independent mea-

surement of λ , we need at least a double Higgs production at the collider. However, this path is fraught with difficulties. Firstly, we need a substantial number of double Higgs events in the collider so that considerable statistics for the precision measurement can be gathered. But most importantly, because the vertices involved in the process are sensitive to the presence of new physics beyond the SM (BSM), we need to take that into account for any possible analyses.

To overcome the first hurdle there are various proposals to build high energy e^+e^- , e^-p and pp machines in the future. We have based our analysis on a proposed e^-p collider on top of the LHC, which would simultaneously operate as a pp collider, and is commonly known as the *Large Hadron Electron Collider (LHeC)* [7, 8]. The choice of $E_e = 60$ to 120 GeV with available proton energy $E_p = 7$ TeV would provide a center of mass (CM) energy $\sqrt{s} \approx 1.3$ to 1.8 TeV at the LHeC. Furthermore, a future extension of the LHeC, to be known as the *Future Circular Hadron Collider (FCC-he)*, is under consideration, where the electron beam from the LHeC would be supplemented with a proton beam of energy 50 TeV [9]. This upgrade will give us a CM energy $\sqrt{s} \approx 3.5$ TeV, considering $E_e = 60$ GeV and $E_p = 50$ TeV. Clearly, the FCC-he would have sufficient energy to probe the Higgs self coupling via double Higgs production.

Fig. 1 shows the production modes of the Higgs pairs due to the resonant and non-resonant configurations in the charged current mode at an e^-p collider. Since we do not yet have any direct measurement of the Higgs self coupling, there can be numerous possible sources of new physics in the scalar sector. Hence, the present article aims to use this energy to not only find the sensitivity of the Higgs self couplings around the SM value, but also the sensitivity of hWW and $hhWW$ couplings by considering all possible Lorentz structures.

Following Refs. [10, 11], the most general Lagrangian which can account for all bosonic couplings, and is the most relevant for the phenomenology of the Higgs sector

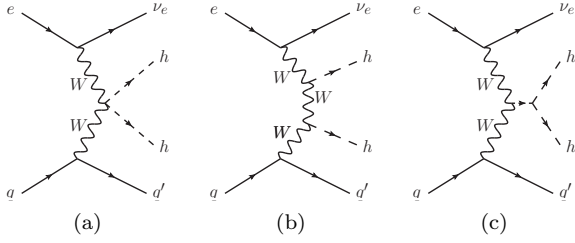


FIG. 1: Diagrams contributing to the process $pe^- \rightarrow hhj\nu_e$. Here $q \equiv u, c, \bar{d}, \bar{s}$ and $q' \equiv d, s, \bar{u}, \bar{c}$ respectively.

at the FCC-he, namely the three-point and four-point interactions involving at least one Higgs field, can be written as:

$$\mathcal{L}_{hhh}^{(3)} = \frac{m_h^2}{2v} (1 - g_{hhh}^{(1)}) h^3 + \frac{1}{2} g_{hhh}^{(2)} h \partial_\mu h \partial^\mu h, \quad (2)$$

$$\begin{aligned} \mathcal{L}_{hWW}^{(3)} = & -\frac{g}{2m_W} g_{hWW}^{(1)} W^{\mu\nu} W_{\mu\nu}^\dagger h \\ & -\frac{g}{m_W} \left[g_{hWW}^{(2)} W^\nu \partial^\mu W_{\mu\nu}^\dagger h + \text{h.c.} \right] \\ & -\frac{g}{2m_W} \tilde{g}_{hWW} W^{\mu\nu} \tilde{W}_{\mu\nu}^\dagger h, \end{aligned} \quad (3)$$

$$\begin{aligned} \mathcal{L}_{hhWW}^{(4)} = & -\frac{g^2}{4m_W^2} g_{hhWW}^{(1)} W^{\mu\nu} W_{\mu\nu}^\dagger h^2 \\ & -\frac{g^2}{2m_W^2} \left[g_{hhWW}^{(2)} W^\nu \partial^\mu W_{\mu\nu}^\dagger h^2 + \text{h.c.} \right] \\ & -\frac{g^2}{4m_W^2} \tilde{g}_{hhWW} W^{\mu\nu} \tilde{W}_{\mu\nu}^\dagger h^2. \end{aligned} \quad (4)$$

Here $g_F^{(i)}$, $i = 1, 2$, and \tilde{g}_F are real coefficients corresponding to the CP-even and CP-odd anomalous vertices respectively. The subscript F denotes the vertices in question, namely hhh , hWW and $hhWW$. The parametrization used for $g_{hhh}^{(1)}$ in Eq. (2) has been done for $g_{hhh}^{(1)}$ to appear as a multiplicative constant to λ_{SM} as in Eq. (1). Thus $\lambda \rightarrow g_{hhh}^{(1)} \lambda_{\text{SM}}$ in the expression for $V(\Phi)$. Clearly, in the SM $g_{hhh}^{(1)} = 1$ with the rest of the anomalous couplings appearing in Eqs. (2)-(4) being zero.

The complete Lagrangian we work with is as follows:

$$\mathcal{L} = \mathcal{L}_{\text{SM}} + \mathcal{L}_{hhh}^{(3)} + \mathcal{L}_{hWW}^{(3)} + \mathcal{L}_{hhWW}^{(4)}, \quad (5)$$

and the most general effective vertices take the form:

$$\begin{aligned} i\Gamma_{hhh} = & -6iv\lambda g_{hhh}^{(1)} \\ & -ig_{hhh}^{(2)} (p_1 \cdot p_2 + p_2 \cdot p_3 + p_3 \cdot p_1), \end{aligned} \quad (6)$$

$$\begin{aligned} i\Gamma_{hW^-W^+} = & i \left[\left\{ \frac{g^2}{2} v + \frac{g}{m_W} g_{hWW}^{(1)} p_2 \cdot p_3 \right. \right. \\ & + \left. \frac{g}{m_W} g_{hWW}^{(2)} (p_2^2 + p_3^2) \right\} \eta^{\mu_2\mu_3} \\ & - \frac{g}{m_W} g_{hWW}^{(1)} p_2^{\mu_3} p_3^{\mu_2} \\ & - \frac{g}{m_W} g_{hWW}^{(2)} (p_2^{\mu_2} p_2^{\mu_3} + p_3^{\mu_2} p_3^{\mu_3}) \\ & \left. - i \frac{g}{m_W} \tilde{g}_{hWW} \epsilon_{\mu_2\mu_3\mu\nu} p_2^\mu p_3^\nu \right], \end{aligned} \quad (7)$$

$$\begin{aligned} i\Gamma_{hhW^-W^+} = & i \left[\left\{ \frac{g^2}{2} + \frac{g^2}{m_W^2} g_{hhWW}^{(1)} p_3 \cdot p_4 \right. \right. \\ & + \left. \frac{g^2}{m_W^2} g_{hhWW}^{(2)} (p_3^2 + p_4^2) \right\} \eta^{\mu_3\mu_4} \\ & - \frac{g^2}{m_W^2} g_{hhWW}^{(1)} p_3^{\mu_4} p_4^{\mu_3} \\ & - \frac{g^2}{m_W^2} g_{hhWW}^{(2)} (p_3^{\mu_3} p_3^{\mu_4} + p_4^{\mu_3} p_4^{\mu_4}) \\ & \left. - i \frac{g^2}{m_W^2} \tilde{g}_{hhWW} \epsilon_{\mu_3\mu_4\mu\nu} p_3^\mu p_4^\nu \right]. \end{aligned} \quad (8)$$

In the above the momenta and indices considered are in the same order as they appear in the index of the respective vertex Γ . For example, in the vertex $\Gamma_{hW^-W^+}$, p_1, p_2 and p_3 are the momenta of h, W^- and W^+ respectively. Similarly, μ_2 and μ_3 are the indices of W^- and W^+ .

In order to probe the sensitivity of these couplings we simulate the charged current double Higgs production channel $pe^- \rightarrow hhj\nu_e$ (shown in Fig. 1), with h further decaying to a $b\bar{b}$ pair, in the FCC-he set up with $\sqrt{s} \approx 3.5$ TeV. The complete signal and background studies for this process can be found in Ref. [12]. For the generation of events we use the Monte Carlo event generator MadGraph5 [13] and further showering, fragmentation and hadronization was done with a *customized* Pythia-PGS [14]. The detector level simulation has been performed with speculated parameters using Delphes [15]. We fixed the factorization and renormalization scale for the signal to be the threshold of the Higgs mass $\mu = \mu_F = \mu_R = m_h = 125$ GeV, with the convolution of CTEQ6L1 parton distribution function. The e^- polarization has been taken to be 80%.

For numerical analysis we take *ad hoc* values of positive and negative couplings in such a manner that the production cross section does not deviate much from the SM value and the shapes could be studied with some physical observable. We have based our simulation on the kinematic criteria and efficiencies adopted in Ref. [12]. These are as follows: (1) At least four b -tagged jets and one additional light jet have been selected in an event with the transverse momenta, p_T , greater than 20 GeV. (2) For *non-b*-jets, the absolute value of the rapidity, $|\eta|$, has been taken to be less than 7, whereas for b -jets it is less than 5. (3) The four b -jets must be well separated

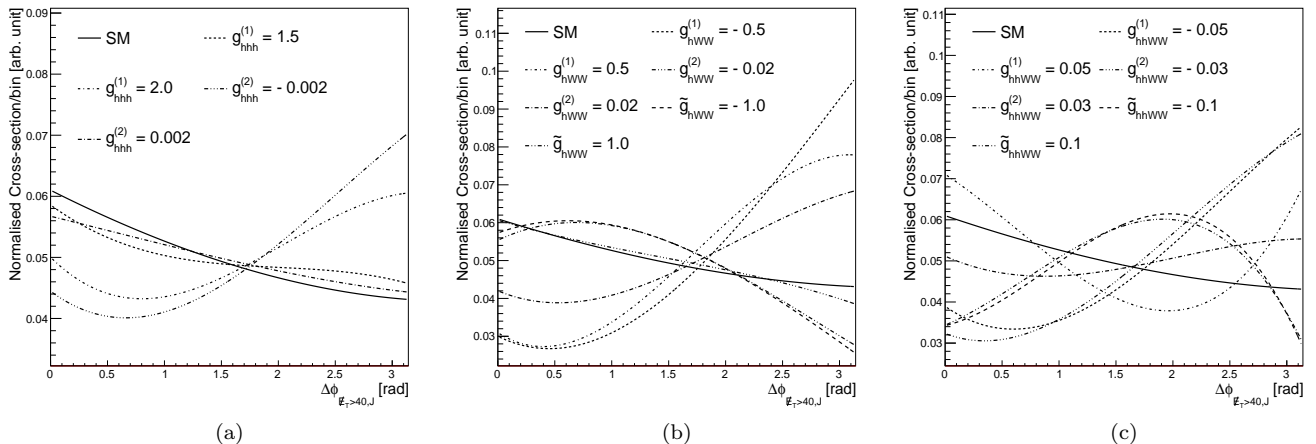


FIG. 2: Azimuthal angle distributions between missing transverse energy, \cancel{E}_T and the forward jet, J , in the SM and with the anomalous hhh , hWW and $hhWW$ couplings.

and hence the distance between any two jets, defined as $\Delta R = \sqrt{(\Delta\phi)^2 + (\Delta\eta)^2}$, ϕ being the azimuthal angle and η the rapidity, were taken to be greater than 0.7, in case of an overlap in the truth matching of the b -tagging. (4) The leptons with $p_T > 10$ GeV were rejected. (5) For the largest p_T forward jet (the *non-b* jet after selecting at least four b -jets), we have taken $\eta_{forward-jet} > 4.0$. (6) The missing transverse energy, \cancel{E}_T , has been taken to be greater than 40 GeV. (7) The azimuthal angle between \cancel{E}_T and the jets are: $\Delta\Phi_{\cancel{E}_T, leadingjet} > 0.4$ and $\Delta\Phi_{\cancel{E}_T, subleadingjet} > 0.4$. (8) To put invariant mass cuts on the b -jets we put the four b -jets into two pairs. The first pair is required to be within 90-125 GeV and the second pair within 75-125 GeV. (9) The invariant mass of all four b -jets is greater than 280 GeV. In all these selections b -tagging efficiency has been taken to be 70%, and the fake rate from the c -initiated jet, or light jet to the b -jet, is 10% and, 1% respectively.

Taking all the above criteria we studied different differential distributions, and this lead to the following observations: (1) p_T has the usual tail behavior, i.e., the number of events are more populated in the higher p_T region with respect to the SM for the chosen values of the anomalous couplings. (2) In case of the η distributions: (a) For the forward jet, particularly for the couplings of hWW and $hhWW$ vertices, η shifts towards the center. The behavior is similar if we increase the CM energy of the collider by increasing E_e to higher values. For hhh couplings the η distribution remains the same as the SM. (b) In case of b -jets, for all values of anomalous couplings, the distribution is populated around the central value of η . (3) For one specific observable, namely $\Delta\phi_{\cancel{E}_T, J}$, between missing transverse energy and the forward jet, the shapes are distinguishable from the SM. This behavior we have shown in Fig. 2, which clearly demands further

detailed discussion here.

Recall that the values of the couplings taken in Fig. 2 are very much *ad hoc* in nature, however, these values were taken only for the purpose of illustration, and in the limit of the couplings going to their SM values the shapes will exactly coincide with the SM and are indistinguishable. The characteristics of the curves also depend on what level of selection cuts we are talking about, but the qualitative differences can be seen at every selection. In this way the exhibited azimuthal angular difference, $\Delta\phi_{\cancel{E}_T, J}$, between missing transverse energy and the forward jet, is a good observable to look for any new physics contribution to these vertices.

Furthermore, we probe the exclusion limits on these couplings as a function of integrated luminosity, \mathcal{L} , with the log-likelihood method described in Ref. [16], using the cross section as an observable. In Fig. 3 we present exclusion plots at 95% C.L. for the anomalous couplings as a function of \mathcal{L} , where the shaded spaces are the allowed region. The exclusion limits are based on the background only observation at the given luminosity. The backgrounds for this analysis are adopted as given in Ref. [12]. Each limit is given by scanning one coupling and fixing the other couplings to their central value, where a 5% systematic uncertainty is taken into account on both signal and background yields. The top most panel shows the exclusion plot for anomalous hhh couplings, the middle one is for the anomalous hWW couplings and the bottom panel shows the exclusion plot for anomalous $hhWW$ couplings.

From Fig. 3 our observations are as follows: (1) If \mathcal{L} is greater than $\sim 0.4 ab^{-1}$ $g_{hhh}^{(1)}$ is only allowed to be positive. If \mathcal{L} reaches about $0.7 ab^{-1}$ the $g_{hhh}^{(1)}$ is restricted from 1 to 2.2. It implies the contribution from $g_{hhh}^{(1)}$ is enhanced over the SM prediction. Once the exclusion is

made at \mathcal{L} greater than $\sim 1.2 ab^{-1}$ the $g_{hhh}^{(1)}$ term is excluded. (2) The limit on $g_{hhh}^{(2)}$ restricts its value to around

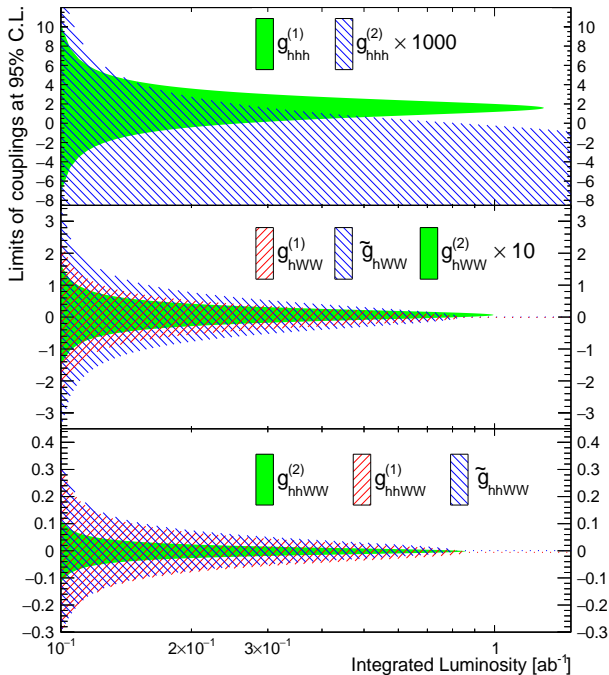


FIG. 3: The exclusion limits on the anomalous hhh , hWW and $hhWW$ couplings as a function of integrated luminosity at 95% C.L. The shaded regions are allowed. The allowed values of $g_{hhh}^{(2)}$ ($g_{hhWW}^{(2)}$) $\sim 10^{-3}$ (10^{-1}) and are hence multiplied by 10^3 (10^1).

10^{-3} , due to its significantly increasing production cross section as a function of the coupling strength. This coupling survives in negative regions when the luminosity is increasing. (3) Among all the anomalous couplings only $g_{hhh}^{(2)}$ can significantly suppress the production cross section below the SM prediction. The other couplings are strongly constrained by the observation because of their very high production cross section. These couplings are also excluded near the same luminosity where $g_{hhh}^{(1)}$ is excluded. All limits are derived by varying only one coupling at a time as mentioned earlier. In combination the $g_{hhh}^{(2)}$ provides the survival probability with respect to other couplings by suppressing the cross section. So the exclusion limit is a strong tool to probe the existence of $g_{hhh}^{(2)}$ and other anomalous couplings.

In this Letter we have extensively explored all the new physics vertices in the double Higgs production channel of an e^-p collider, namely hhh , hWW and $hhWW$, in a model independent way. The authors of Ref. [10] have shown in a similar study that the azimuthal angle $\Delta\phi_{\vec{E}_T, J}$ is a very good probe of anomalous hWW couplings in charged current single Higgs production at the LHeC. Though both the papers considered have similar

Lorentz structures for the CP-even/odd hWW couplings we can not compare our results directly with theirs because: (a) Their final states are $hj\nu_e$ consisting of only one diagram with the hWW coupling playing the all important role, whereas our final states are $hhj\nu_e$ where we have other couplings also in addition to theirs in more than one diagram. (b) They derived the exclusion on $\Delta\phi_{\vec{E}_T, J}$ in an accessible region of single Higgs production. However, in our case, we have taken $\Delta\phi_{\vec{E}_T, J}$ for probing distribution characteristics, but used the production cross section as the exclusion observable. Still, the overall sensitivity for the values of these hWW couplings have the same order of magnitude in the accessible region of \mathcal{L} for both the single and double Higgs production mode at an e^-p collider. We further observe that: (a) Though hWW couplings can be probed at the LHeC, the other two couplings appearing in our case need still higher CM energy, that is, we need to go to the FCC-he to probe them. (b) The two couplings appearing for the hhh vertex have very different Lorentz structures. While $g_{hhh}^{(1)}$ is just a multiplicative constant to λ_{SM} , $g_{hhh}^{(2)}$ accompanies a new momentum dependent structure. As a result, $g_{hhh}^{(1)}$ is of the same order of magnitude as that of the λ_{SM} , but $g_{hhh}^{(2)}$ is $\sim 10^{-3}$ less because the cross section grows very fast with the increase in absolute value of this coupling. (c) One important aspect of di-Higgs production in this type of collider is that one can measure the sensitivity of $hhWW$ couplings also. In our analysis, since the CP-even (odd) coupling $g_{hhWW}^{(1)}$ (\tilde{g}_{hhWW}) has similar Lorentz structures, the sensitivity in the exclusion plot has almost the same order of magnitude. However, the structure of $g_{hhWW}^{(2)}$ allows a comparatively narrower region of values. We conclude that a CM energy available at the FCC-he facility at an integrated luminosity $\sim 0.4 ab^{-1}$ would allow us to probe any new physics in the double Higgs channel at e^-p colliders up to a satisfactory level.

One curious question here is to know what happens once we elevate E_e to higher values. Without going into details we can mention that on increasing E_e to 120 GeV the signal and dominant background production cross sections enhance by ~ 2.2 and ~ 1.7 times, with respect to that at $E_e = 60$ GeV, respectively. As a result, the cut efficiency for the selection of 4 b -jets and 1 light jet is affected, but for other cuts described previously (invariant mass, \vec{E}_T , $\eta_{forward-jet}$ and $\Delta\phi_{\vec{E}_T, J}$) it remains intact. This leads to an enhancement of ~ 2.5 and ~ 2.7 times on signal and dominant background events respectively. In other words, we simply need only 40% luminosity as that of $E_e = 60$ GeV to get the same statistics and results.

We acknowledge the LHeC group members for their fruitful discussions within the bi-weekly meetings, especially Masahiro Kuze and Masahiro Tanaka. RI acknowledges the DST-SERB supported research project SRIS2/HEP-13/2012 for partial financial support.

-
- * Electronic address: mukesh.kumar@cern.ch
† Electronic address: xifeng.ruan@cern.ch
‡ Electronic address: rashidul.islam@cern.ch
§ Electronic address: alan.cornell@wits.ac.za
¶ Electronic address: max.klein@desy.de
** Electronic address: uklein@hep.ph.liv.ac.uk
†† Electronic address: bruce.mellado.Garcia@cern.ch
- [1] G. Aad *et al.* [ATLAS Collaboration], Phys. Lett. B **716**, 1 (2012).
[2] S. Chatrchyan *et al.* [CMS Collaboration], Phys. Lett. B **716**, 30 (2012).
[3] F. Boudjema and E. Chopin, Z. Phys. C **73**, 85 (1996).
[4] E. Asakawa, D. Harada, S. Kanemura, Y. Okada and K. Tsumura, Phys. Rev. D **82**, 115002 (2010).
[5] A. Djouadi, W. Kilian, M. Muhlleitner and P. M. Zerwas, Eur. Phys. J. C **10**, 45 (1999).
[6] A. Djouadi, W. Kilian, M. Muhlleitner and P. M. Zerwas, In *2nd ECFA/DESY Study 1998-2001* 791-811 [hep-ph/0001169].
[7] J. L. Abelleira Fernandez *et al.* [LHeC Study Group Collaboration], J. Phys. G **39**, 075001 (2012).
[8] <http://lhec.web.cern.ch/>
[9] <http://ph-news.web.cern.ch/content/fcc-he-renaissance-deep-inelastic-scattering-cern>
[10] S. S. Biswal, R. M. Godbole, B. Mellado and S. Raychaudhuri, Phys. Rev. Lett. **109**, 261801 (2012).
[11] A. Alloul, B. Fuks and V. Sanz, JHEP **1404**, 110 (2014).
[12] M. Kumar, X. Ruan, R. Islam, A. S. Cornell, M. Klein, U. Klein and B. Mellado, Draft in preparation.
[13] J. Alwall, M. Herquet, F. Maltoni, O. Mattelaer and T. Stelzer, JHEP **1106**, 128 (2011).
[14] T. Sjostrand, S. Mrenna and P. Z. Skands, JHEP **0605**, 026 (2006).
[15] J. de Favereau *et al.* [DELPHES 3 Collaboration], JHEP **1402**, 057 (2014).
[16] G. Cowan, K. Cranmer, E. Gross and O. Vitells, Eur. Phys. J. C **71**, 1554 (2011) [Eur. Phys. J. C **73**, 2501 (2013)].